Z. Phys. Chem. **224** (2010) 1247–1260 / **DOI** 10.1524/zpch.2010.6150

Aqueous Phase Reactivity of Nitrate Radicals (NO_3) Toward Dicarboxylic Acids

By Ph. G. de Sémainville, B. D'Anna, and Ch. George*

Université de Lyon 1, CNRS, UMR5256, IRCELYON, Institut de recherches sur la catalyse et l'environnement de Lyon, Villeurbanne, F-69626, France

Dedicated to Prof. Dr. Reinhard Zellner on the occasion of his 65th birthday

(Received December 9, 2009; accepted March 21, 2010)

Nitrate Radical / Kinetics / Dicarboxylic Acids

Laser photolysis technique was used to study the reactivity of nitrate radical towards four dicarboxylic acids. The temperature dependence of the reactions was investigated in the range from 278K to 318K. The effect of the acid-base equilibrium was examined by measuring the activation parameters of the dissociated and undissociated acids at different pH. For droplets or aerosols under moderate acidic conditions, the charge exchange reaction at the carboxylate group might compete with the oxidation by the hydroxyl radical. On liquid particles enriched in nitrate (such as a deliquescent ammonium nitrate), the lifetime of carboxylic groups towards the NO_3 radical may be as short as few hours (or less).

1. Introduction

Radicals are key compounds in a variety of chemical processes including the natural degradation of pollutants. This is often observed in the atmosphere which can be regarded as a giant chemical reactor. As an example, the oxidation capacity of the atmosphere is mainly governed by the presence of radicals such as OH or NO_3 which will react will almost all organic pollutants. Such oxidation cycles will lead, among other, to the photochemical production of ozone which is currently fairly well understood.

Furthermore, our society is facing a changing atmosphere as a response to a man-made anthropogenic pressure and these changes are far from being well understood. Over the last decades, aerosols and clouds have been considered as the "least predictable" object in our understanding of the atmospheric and climate

---

* Corresponding author. E-mail: christian.george@ircelyon.univ-lyon1.fr

systems. On the global scale, atmospheric aerosols are recognized as having a major impact on the Earth's climate through direct and indirect radiative forcing.

The organic component of aerosols may affect climate in multiple ways: organic compounds can act as surfactants and by their limited solubility modulate aerosol interactions with water vapour, and hence, hygroscopic growth and cloud condensation nuclei (CCN) activity. A major effort has recently been devoted to the understanding of organic aerosol formation, composition and physico-chemical properties. Aerosols have an atmospheric lifetime that can reach one or two weeks. It is therefore necessary to investigate their chemical transformations in the atmosphere. Chemical processes may lead to changes in both climate and health effects of the aerosols due to variation in their composition, optical properties and interaction with water.

For instance, Saxena and Hildeman [1] showed that freshly emitted aerosols are made of relatively non-oxidized compounds with hydrophobic properties, while aged aerosols becomes more hydrophilic and contain more oxygenated species/functionalities. Among the latter, dicarboxylic acids can made up to 50% of the aerosol mass (with respect the soluble fraction). Carboxylic and especially dicarboxylic acids are therefore key compounds that may affect aerosol lifetimes and also cloud formation potential (both of them are intimately linked to the changing climate).

Such carboxylic and dicarboxylic acids may be produced in the atmosphere in a variety of gas phase reactions including ozonolysis of long chain fatty acids, aromatics, etc… But the atmosphere is far from being a purely homogeneous media and several processes may occur in clouds, which are ubiquitous. Each individual cloud droplet acts a small aqueous chemical reactor in which soluble pollutants will be processed. Ervens and Kreidenweis [2] showed in a modelling study that short chain dicarboxylic acids (mainly oxalic acid) will be produced in cloud.

Nevertheless, the atmospheric fate of such acids is still unclear as many fundamental parameters have not been studied so far. In fact, kinetic and mechanistic data on the reactivity of dicarboxylic acids are not well established. Similar to the gas phase, chemical conversion within a cloud droplet is driven by radicals (again such as OH or NO_3) [3,4] but the possible reaction pathways are manifold. As in the gas phase, H-abstraction is a possible reaction pathway but in the aqueous phase, organic acids may also undergo acid-base dissociation and the resulting ions may in addition initiate charge exchange reactions. Therefore, the knowledge gained from gas phase chemistry should not be straightforwardly transferred to the atmospheric aqueous phase, as reactivity and mechanisms may be pH dependent. This latter parameter may be especially important in the marine environment were the pH of deliquescent aerosol span over a quite wide dynamic range influenced by the uptake or release of acids [5,6].

Due to the importance of the nitrate radical for chemical transformation in clouds, we studied the reactivity of the NO_3 towards four different dicarboxylic acids i.e., oxalic, malonic, mesoxalic and succinic acids as a function of pH and temperature by means of a laser photolysis technique. In the following sections we will describe experimental layout, followed by the results and the discussion, highlighting some features of the reactivity of the selected dicarboxylic acids.

2. Experimental section

Experimental details have been already published elsewhere [7–10], therefore only a brief description is given below.

2.1 Nitrate radical generation

The generation of the nitrate radical was achieved using two different methods. In the first method (A), the NO_3 radicals were produced by the laser photolysis at 266 nm of an aqueous nitrate solution at pH = 0.5 according to:

$$NO_3^- + H^+ + h\nu \rightarrow NO_2^\bullet + OH^\bullet \tag{R1}$$

$$HNO_3 + OH^\bullet \rightarrow NO_3^\bullet + H_2O \tag{R2}$$

The method requires relatively high acidic conditions in order to produce enough molecular nitric acid for reaction (R2) to occur at a reasonable rate. On the other side the advantage is due to the limited number of short lived radicals as precursors (i.e., OH). Accordingly the reaction sequence (R1–R2) is a relatively clean source of radicals but limited to acidic conditions. Typically the radicals were produced at pH = 0.5 with $NaNO_3$ concentrations of 0.5 mol L^{-1}.

In the second method (B), the NO_3 radicals were produced through laser-flash photolysis of peroxodisulfate in presence of nitrate anion at 355 nm according to:

$$S_2O_8^{2-} + h\nu \rightarrow 2SO_4^{-\bullet} \tag{R3}$$

$$SO_4^{-\bullet} + NO_3^- \rightarrow SO_4^{2-} + NO_3^\bullet \tag{R4}$$

Using reactions (R3) and (R4) implies a delay longer than in method A to achieve complete formation of the nitrate radicals. This time gap depends on Laser fluence and reactant concentrations. Therefore, depending on the experimental conditions, the decay of the nitrate radical may not necessarily be of first order during the few microseconds following the laser discharge. Thus care must be taken during NO_3 radical analysis ensuring that its decay occurs/is evaluated after complete production of NO_3. This was achieved under following conditions: $[NaNO_3] = 0.1 - 0.5$ mol L^{-1} and $[Na_2S_2O_8] = 0.1$ mol L^{-1}.

2.2 LASER photolysis set-up

A Continuum Surelite II operated at 266 or 355 nm was used as the photolysis source. Under optimum conditions, this laser produces a pulse half-width of 3 ns and a beam cross-sectional diameter of 8 mm in conjunction of an output of 100 mJ per pulse at 266 nm and 200 mJ at 355 nm. This beam was then expanded to irradiate uniformly the photolysis cell (described in more details below) over a rectangle of ca. 1×3 cm^2 (height × width).

Transient species produced by the pulsed laser beam were monitored by means of time resolved absorption spectroscopy. A He-Ne laser (LASOS, LGK7654–8), with an output wavelength of 633 nm and a power of 25 mW was used as the analyzing light. The light escaping the photolysis cell (described below) was fed, through an interference filter at 633 nm, onto the active surface of an amplified photodiode (FEMTO, HCA-S-200M-SI). The rise time (5 to 95%) of the amplified photodiode was below 2 ns. The transient optical absorption signal produced by the laser beam was subsequently collected by a Tektronix oscilloscope (type 2430A). Up to 16 single shots were averaged before transmitting to a computer and the photolysis cell content was renewed between each laser pulse. We ensured that single and averaged signals lead to the same kinetic determination.

2.3 Teflon AF photolysis cell

The centrepiece of the experimental set-up is a Liquid Core Waveguide (LCW) made of Teflon AF 2400 (BioGeneral, San Diego, CA). Such type of material has been shown to exhibit excellent optical properties such as high optical clarity (at $\lambda \leq 200$ nm more than 80% of light is transmitted through a 220 μm thick film of the polymer described above) and very low refractive index (i.e., $n = 1.29$ for Teflon AF 2400 grades). As a result, such type of tubing once filled with water will conduct light. The Teflon AF 2400 guide had an inner and outer diameter of 0.8 mm and 1.0 mm, respectively, a length of 50 cm with an inner volume of 0.25 mL. This very small liquid volume represents the major advantage of the waveguides compared to standard White cells.

The highly flexible Teflon AF 2400 tubing was loosely coiled (less than 3 cm diameter) and placed in the laser beam path. The NO_3 radicals were generated within the LCW following the laser flash of the precursors as discussed above. As the waveguide was used as a coil, no concentration gradient could build up along the waveguide length. However, non-uniform nitrate radical concentration can be produced if the laser fluence on the coil is not uniform. We prevent shielding of the front and back side of the waveguide by placing it inside a small box ($1 \times 3 \times 3$ cm^3 height × width × depth) with inner walls coated by aluminium foil. This ensured a better irradiation of the waveguide even if the fluence could not be measured. Consequently we made sure that all kinetics studied were unimolecular (after completion of NO_3 generation as stated before).

The solution content of the Teflon photolysis cell was probed by focusing the output of the He-Ne laser on the entry of an unpolished 500-μm diameter fused silica optical fibre. Then, the light was allowed to escape the solid optical fibre and collected in the liquid core waveguide. Again, the Teflon AF tubing conducted the light up to its end where another fused silica optical fibre (located in the liquid) collected most of this transmitted light to the amplified photodiode. In this way, the measured signal is integrated (or averaged) over the full length of the waveguide. As the observed decays were first order, this averaging allowed the determination of the rate constants even in the unlikely situation where the NO_3 concentration was not uniform along the waveguide length.

2.4 Reagents

Solutions were prepared from following chemicals (used without further purification): $Na_2S_2O_8$ (Aldrich, 98%), $NaNO_3$ (Aldrich, 99%), nitric acid (Aldrich 1 mol L^{-1}), perchloric acid (Aldrich 70%), oxalic acid (Riedle de Haën, 99%), malonic acid (Fluka, 99%), succinic acid (Fluka, 99%) and sodium mesoxalate, monohydrate (Fluka, 98%). Water was taken from an 18MΩ purification system (Millipore). In some test experiments, we used oxygen free solutions, which led to the same results as non-degassed water.

3. Results

3.1 Kinetic data

The methodology described above has been applied to study the NO_3 radical reactions with oxalic ($pKa_1 = 1.23$; $pKa_2 = 4.19$), malonic ($pKa_1 = 2.83$; $pKa_2 = 5.69$), mesoxalic ($pKa_1 = 1.60$; $pKa_2 = 3.90$) and succinic ($pKa_1 = 4.19$; $pKa_2 = 5.48$) acids as a function of temperature and pH. Figures 1 and 2 show raw data of mesoxalic acid demonstrating the measured kinetics are first order (Figure 2). Bimolecular plots from which the second order rate reactions were derived are given in Figure 3. The kinetic data, as well as the available literature values, are summarized in Table 1 at a 2σ error level.

The rate constants were measured as a function of temperature in the range from 278K to 318K for malonic (pH = 4.26), mesoxalic and succinic acid, from 278K to 298K for oxalic acid (because of thermal degradation of the oxalate) and between 278K and 308K for malonic acid at pH = 8 (adjusted with NaOH). Figure 4 shows typical Arrhenius plots for mesoxalic acid at pH = 0. Table 1 also lists Arrhenius parameters for all the reactions studied here i.e., pre-exponential factor (A) and activation energies (Ea) along with the parameters derived from the Eyring equation i.e.,

$$k = \frac{k_B T}{h} e^{-\Delta G^{\neq}/RT} \tag{E1}$$

namely following activation parameters:

$$\Delta S^{\neq} = R[\ln(A) - \ln(\frac{k_B T}{h}) - 1] \tag{E2}$$

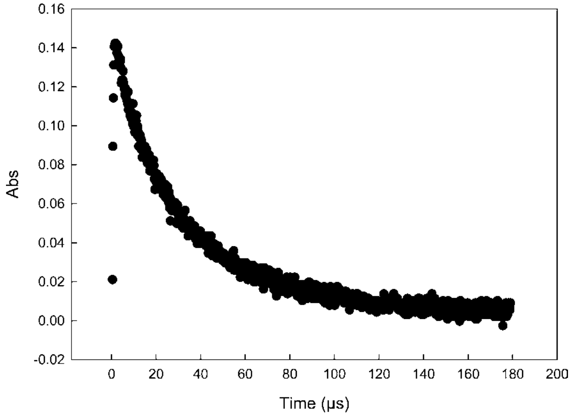

Fig. 1. Experimental decay, absorbance versus time, for mesoxalic acid at pH = 0 (method A at 266nm).

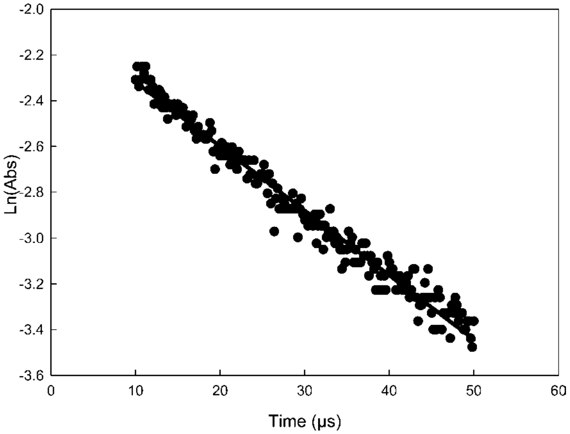

Fig. 2. First order kinetic plot for mesoxalic acid at pH = 0 (method A at 266nm).

$$\Delta H^{\neq} = E_a - RT \tag{E3}$$

$$\Delta G^{\neq} = \Delta H^{\neq} - T\Delta S^{\neq} \tag{E4}$$

Table 1 also shows the pH dependence of the measured kinetic parameters. Obviously dicarboxylic acids have two pKas therefore, depending on the pH, the chemistry of the neutral (or molecular), the singly and doubly charged anions of the acid are investigated. And as can be clearly seen in Table 1, the protonation/deprotonation degree strongly influences the reactivity of the acid.

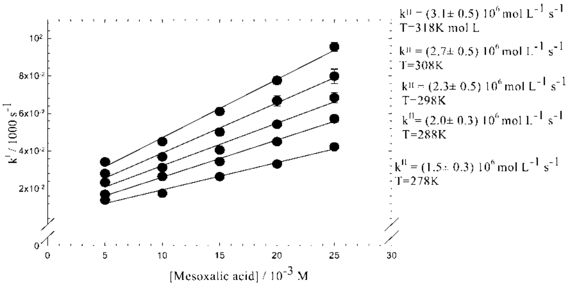

Fig. 3. Bimolecular plots for mesoxalic acid at pH = 0 (method A at 266nm) at different temperatures.

Table 1. Summary of kinetic and thermodynamic data for the investigated NO_3 reactions in aqueous solution measured in this study.

Compound	n_H^*	$k_{2nd.298K}$ $[M^{-1}s^{-1}]$	A $[M^{-1}s^{-1}]$	E_A [kJ/mol]	$\Delta G^\ddagger$ [kJ/mol]	$\Delta H^\ddagger$ [kJ/mol]	$\Delta S^\ddagger$ [J/mol·K]	BDE^{**} [kJ/mol]	Method
Malonic acid	2	$(5.1\pm0.5)\cdot10^4$						400^{24}	B pH 0.3
Malonate monoanion	2	$(5.6\pm2.1)\cdot10^6$	$(5.0\pm0.6)\cdot10^{11}$	28±7	34±8	26±7	−(29±3)	–	B pH 4.26
Malonate dianion	2	$(2.3\pm0.5)\cdot10^7$	$(6.3\pm0.8)\cdot10^{11}$	25±8	31±9	23±8	−(27±3)	–	B pH 8
Mesoxalic acid	0	$(1.7\pm0.5)\cdot10^6$	$(5.1\pm0.4)\cdot10^8$	13±4	37±6	11±4	−(86±6)	–	A pH 0
Mesoxalate monoanion	0	$(2.3\pm0.4)\cdot10^7$						–	B pH 2.7
Mesoxalate dianion	0	$(4.9\pm1.5)\cdot10^7$	$(1.4\pm0.1)\cdot10^{12}$	26±4	28±5	23±4	−(21±1)	–	B pH 8
Oxalic acid	0	$<5\cdot10^4$						–	
Oxalate monoanion	0	$(4.4\pm0.2)\cdot10^7$						–	B pH 2.7
Oxalate dianion	0	$(2.2\pm0.8)\cdot10^8$	$(2.2\pm0.2)\cdot10^{12}$	23±6	25±7	20±6	−(17±2)	–	B pH 8
Succinic acid	4	$(5\pm5)\cdot10^3$						398^{24}	B pH 0.3
Succinate monoanion	4	$(1.1\pm0.2)\cdot10^7$						–	B pH 4.2
Succinate dianion	4	$(1.8\pm0.2)\cdot10^7$	$(6.2\pm0.6)\cdot10^{11}$	26±3	32±4	23±3	−(27±3)	–	B pH 8

* n_H = number of the identically most easily abstractable H-atoms in the molecule;

** for C-H bonds.

In aqueous solutions, these acids will react either through an H-abstraction channel or by a charge exchange reaction.

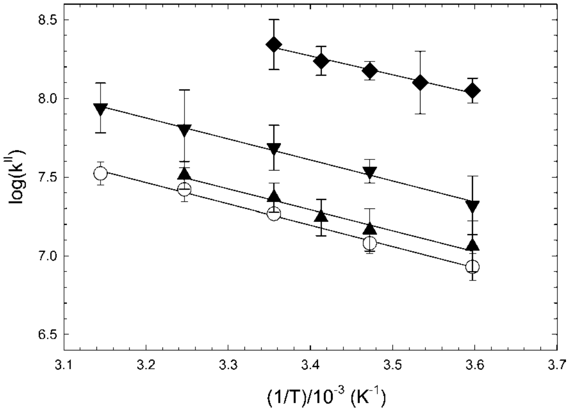

Fig. 4. Arrhenius plots for the reactions with ○ succinate dianion, ▲ malonate dianion,▼ mesoxalate dianion, oxalate dianion.

3.2 Reactivity of the acid in its neutral form

Under acidic conditions (i.e., typically one unit below the first pKa of the acid) only the molecular form of the acid should be present in solution (with maybe traces of the singly charged anion). Under such condition the possible reaction pathway is an H-abstraction either from a C-H or an O-H bond.

From Table 1, it can be seen that the reaction coefficients of the protonated acids span several orders of magnitude (from below 10^4 up to 10^6 L mol^{-1} s^{-1}) highlighting a quite different reactivity of the various acids. For oxalic acid and at pH below 1, the only abstractable H atom is from the carboxylic group. Yang *et al.* [11] measured a rate constant of (2.4±0,2) 10^4 L mol^{-1} s^{-1} by pulse radiolysis in 2 mol L^{-1} nitric acid. If the reaction occurs by an H-abstraction, we do not expect the reactivity to be strongly pH dependent. But as shown in Figure 5, a very strong pH dependence of the measured rate constants is observed which points towards an important influence of traces of singly charged species especially around pH = 1. If we do assume that the measured reactivity is due to both the neutral (AH) and singly charged (A^-) forms of the acid then the following equation may apply:

$$k_{tot}([AH]+[A^-]) = k_{AH}[AH]+k_{A^-}[A^-]. \qquad \text{(E5)}$$

where k_{tot} is the measured overall rate constant i.e., a combination of k_{AH} and k_{A-} which are the rate constants for the molecular form and its monoanion. Assuming that the reactivity of the neutral acid AH can be neglected and using the relationship between pH and pKa, one can obtain the following relationship:

$$\log(k_{tot}(1+10^{pH-pKa})) = \log(k_{A^-})-pKa+pH \qquad \text{(E6)}$$

As shown by Figure 5, this linear relationship is indeed observed, validating the hypothesis that the neutral acid is quite unreactive toward the nitrate radical.

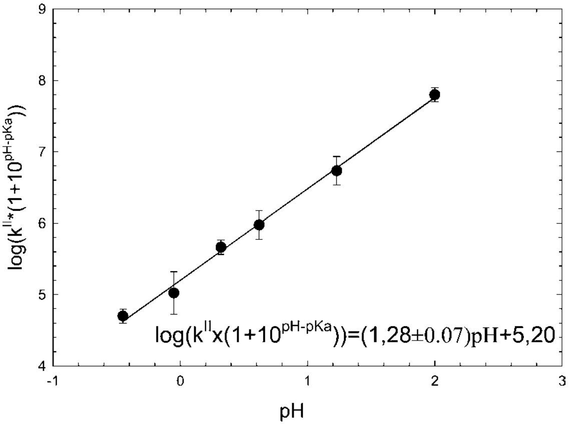

Fig. 5. Plot of $\log(k^{II}x(1+10^{pH-pK_a}))$ as a function of pH for oxalic acid at 298K (according to equation E6).

The useful pH range is limited here by the pKa of the acid (i.e., to have only traces of the dissociated acid). We therefore concluded that H-abstraction from the carboxylic function can be neglected in aqueous solutions which is in agreement with the quite high O-H bond dissociation energy measured (BDE = 468 kJ mol^{-1} [12]). In conclusion, for oxalic acid, the reactivity of the mono anion dominates even at pH below 1, despite being present at very low concentration, explaining also the measurements by Yang *et al.* [11]. Therefore there is no H abstraction channel for oxalic acid. This is in agreement with Neta *et al.* [13,14] who studied the reactivity of H atoms toward a series of carboxylic acids and also showed that there is no H abstraction from oxalic acid.

Malonic acid has two C-H bonds between two carboxylic functions, accordingly H abstraction is possible and even favoured by the proximity of the -COOH groups. Therefore, the neutral form of the malonic acid is more reactive than the oxalic acid (where no reaction is observed at all) and has a rate constant of (5.1±2.0) 10^4 L mol^{-1} s^{-1} comparable to that measured for a similar compound as dimethylmalonate [8].

Succinic acid differs from malonic acid just by one additional CH_2 group and the measured rate constant was (5±5) 10^3 L mol^{-1} s^{-1}, an order of magnitude lower than for malonic acid. This can be speculatively explained by a less efficient inductive effect of the –COOH group.

Interestingly, under acidic conditions, the most reactive acid is the mesoxalic one, with a measured rate constant of (2.27±0.50) 10^6 L mol^{-1} s^{-1} at pH = 0. As for oxalic acid, this value is influenced by the chemistry initiated by traces of mesoxalic monoanion (calculated to be less than the molecular form by a factor of 40 at pH = 0). Taking advantage of the kinetics measured at intermediate pH (see below and Table 1), we can subtract the influence of the singly

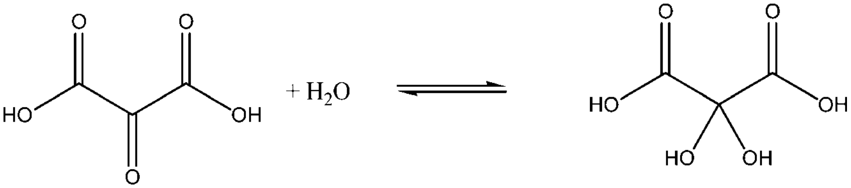

Scheme 1.

charge compound as being $2.3\times10^7/40$ or 5.8×10^5 L mol^{-1} s^{-1}. The corrected rate constant is then (1.7±0.5) 10^6 L mol^{-1} s^{-1}. This acid differs from the previous ones as it undergoes gem-diol reactions according to Scheme 1.

At low pH, the gem-diol structure is strongly favoured depending also on the temperature [15]. At pH = 1.7, Schuchmann *et al.* [15] showed that the ratio of diol to the carbonyl structure is larger than 100. Therefore we will consider that under acidic conditions only the diol is present in the aqueous solution. In this case, there is no abstractable H atom (as there is no C-H bond and the O-H bond is too strong to react with NO_3).

Interestingly, a similar high reactivity has also been observed for pyruvic acid which also undergoes gem diol equilibrium [7]. Therefore, one might wonder if this feature is characteristic for a carbon linked to two OH groups, as hypothesized by Gilbert et al.[16], leading an electron transfer to one OH function. From the data reported here, we can only speculate about the existence of this pathway.

3.3 Reactivity at intermediate pH

At intermediate pH values i.e., at pH between the two pKas of the acids, the mono acid dominates and both H abstraction and electron transfer are possible. And as observed by Exner *et al.* [17], the reactivity increases drastically. Interestingly, while at low pH the rate constants were spanning over quite a large range, at intermediate pH all acids exhibit similar reactivity around 10^6–10^7 mol L^{-1} s^{-1} (see Table 1), even for mesoxalic acid which was "an outlier" at low pH.

For oxalic acid, rate constants at 298 K listed in Table 1 are in agreement with those previously reported by Yang *et al.* [11] and Zellner *et al.* [18] who reported the activation energies at pH = 4.

The two pKas of succinic acid are very close and it is consequently very difficult to measure the reactivity of the corresponding monoanion. The experiments were therefore conducted at pH = 4.2 close to the first pKa, to limit the influence of the dianion. The derived rate coefficient was (6.6±1.8) · 10^6 L mol^{-1} s^{-1}, from which the contribution of the dianion (see below) i.e., $1.8\cdot10^7\text{x}10^{\mathrm{pH}-\mathrm{pKa2}}$ which equals $9\cdot10^5$ L mol^{-1} s^{-1} was subtracted. At pH equal to the first pKa the monoanion concentration is half of the total acid concentration, this last correction leads to the reported rate constant of $(1.1\pm0.2)\ 10^7$ L mol^{-1} s^{-1}.

3.4 Reactivity at high pH

At high pH (i.e., above the second pKa), the acids are fully deprotonated and the dianions dominate and under such condition the reactivity further increases, as can be seen from Table 1.

The longest carbon chain is the one of the succinic acid, where the two carboxylic functions should have a weaker interaction than for shorter dicarboxylic acids. For succinic acid the reactivity of the dianion is roughly the double (within the experimental errors) of the reactivity of the monoanion (see Table 1). This can be easily explained by the doubling of the carboxylate group concentration. In other words, per $–COO^-$ function the reactivity at intermediate and high pH are similar underlining certainly a similar reaction pathway i.e., a charge exchange reaction from the carboxylate function.

However, the ratio between the measured rate constants for the monoanion and dianion decreases for the other acids, and the oxalate dianion showed the highest reactivity. This highlights the fact that the $–COO^-$ groups do stronger interact leading to an increase in reactivity. The activation parameters for this reaction with the oxalate dianion have been previously reported by Zellner *et al.* [18] at pH = 9. The measured activation energies are in reasonable good agreement with this previous study.

4. Atmospheric implications

As discussed above, the H-abstraction mechanism is a possible reaction channel, while still minor in most cases, for the undissociated carboxylic acids (i.e., under acidic conditions), leading to the formation of HNO_3. Nevertheless electron transfer dominates as soon as the pH reached the first pKa of the acid. These reactions are then in competition with photolysis processes, gas phase chemistry as well as the uptake into atmospheric aqueous droplets or particles [19–21].

From the measured rate constants, it becomes possible to evaluate the lifetime of an organic compound in solution with respect to a given radical, simply using the following equation:

$$\tau = \frac{1}{k_{2nd} \cdot [radical]} \tag{E7}$$

The calculated lifetimes are listed in Table 2 under two extreme scenario i.e., under acid (urban pollution) and near neutral conditions (rural or marine case) applying the NO_3 concentrations of atmospheric aqueous phase reported by Herrmann *et al.*, 2005 [22]. It must be underlined that OH and NO_3 do not have the same diurnal cycle and therefore reactions with NO_3 radical will be important for the degradation of carbonyl compounds at very low actinic fluxes [23].

Table 2. Aqueous phase rate constants as well as tropospheric lifetimes in urban (acidic conditions) and remote (neutral conditions) areas of the studied compounds. (a) from Ervens *et al.* [2]; (b) from Electronic Supplementary Material from Herrmann *et al.*[22]; (c) calculated from Ervens *et al.* [2];. (d) from Walling *et al.* [25];(e) from Logan [26]; (f) from Gligorovski *et al* [27].

	Rate constant [M^{-1} s^{-1}]		tropospheric lifetimes τ [h] – aqueous phase			
	Aqueous phase		rural		urban	
	k_{OH}	k_{NO_3}	$[OH^\bullet]$ $1.5 \cdot 10^{-13}$ M	$[NO_3^\bullet]$ $1.0 \cdot 10^{-14}$ M	$[OH^\bullet]$ $1.0 \cdot 10^{-14}$ M	$[NO_3^\bullet]$ $1.7 \cdot 10^{-13}$ M
Malonic acid	$1.4 \cdot 10^{6(d)}$	$5.1 \cdot 10^4$	–	–	$2.0 \cdot 10^4$	$3.2 \cdot 10^4$
Malonate(*)	$1.7 \cdot 10^{8(d)}$	$1.4 \cdot 10^7$	10.9	$2.0 \cdot 10^3$	–	–
Mesoxalic acid	$1.8 \cdot 10^{8\ (f)}$	$2.3 \cdot 10^6$	–	–	$1.5 \cdot 10^2$	$7.1 \cdot 10^2$
Mesoxalate	$1.2 \cdot 10^{8\ (f)}$	$4.9 \cdot 10^7$	15.4	$5.7 \cdot 10^2$	–	–
Oxalic acid (**)	$2.4 \cdot 10^{7(c)}$	$8 \cdot 10^5$	–	–	$1.2 \cdot 10^3$	$2.0 \cdot 10^3$
Oxalate	$1.6 \cdot 10^{8(a)}$	$2.2 \cdot 10^8$	11.6	$1.3 \cdot 10^2$	–	–
Succinic acid	$1.1 \cdot 10^{8\ (a)}$	$5.0 \cdot 10^3$	–	–	$2.5 \cdot 10^2$	$3.3 \cdot 10^5$
Succinate(*)	$5.0 \cdot 10^{8\ (a)}$	$1.4 \cdot 10^7$	3.7	$2.0 \cdot 10^3$	–	–

(*) Due to the high pKa values of these acids (malonic, pKa = 5.69: succinic, pKa = 5.48 respectivement), an average reactivity between the singly and doubly compounds has been calculated.

(**) For oxalic acid, as its reactivity is governed by the singly compound the measured rate constant at pH = 6 has been arbitrarily taken.

Table 2 clearly shows that the OH reaction dominates in the urban scenario (acidic conditions), due to the higher reactivity of OH radical, which is partly compensated by higher NO_3 concentration. So in most cases the OH radical is the major oxidant, but the nitrate radical gains importance near neutral conditions. Interestingly, under neutral conditions, when electron transfer reaction dominates the reaction between the NO_3 radical and the dicarboxylic acids, the nitrate chemistry will introduce a new chemical pathway in which decarboxylation may occur. For example, in the marine environment, this may lead to organic compounds escaping more easily the liquid phase i.e., the wet aerosols will act as a VOC source.

5. Conclusions

This work addressed the oxidation of several dicarboxylic acids by the nitrate radical using a newly developed experimental technique. The experimental approach described herein takes advantage of the novel Teflon AF 2400 material. The physical nature of such tubing allows for the construction of photolysis reaction cells with very low volumes and long optical path lengths. We have successfully applied such photolysis cell to the measurement of the rate coefficients for the liquid phase reaction of the nitrate radical with oxalic, malonic, mesoxalic and succinic acids as a function of pH and temperature.

These acids, depending upon the pH, may react with the nitrate radical through different pathways i.e., either H abstraction (at all pH at the C-H bond) and charge exchange reaction (for pH above the first pKa). Clearly when comparing the kinetics, the reaction is much faster under alkaline conditions strongly suggesting that the charge exchange transfer is much faster than the H abstraction. Also when going from the singly and doubly charged species, the rate constant roughly doubles following the change in the COO^- concentration.

For not (too) acidic pH of droplets and/or aerosols the charge exchange reaction at the carboxylate functional group might compete with the oxidation by hydroxyl radical. Also, for liquid particles enriched in nitrate (such as a deliquescent ammonium nitrate), the lifetime associated to a carboxylic acid being oxidised by NO_3 in may be as short a few hours (or less). Accordingly, one could speculate that any fatty acid (such as oleic acid) acting a surfactant deposited on such a deliquescent particle may be oxidised in both phase i.e., by ozone from the gas phase and by the nitrate radical within the particle. In addition, a charge transfer reaction on the carboxylate function may initiate a decarboxylation process and desorption from the particle of volatile hydrocarbons.

Acknowledgement

Support of this work by the Programme National de Chimie Atmosphérique (PNCA) from the CNRS is gratefully acknowledged along the Ph-D grant for PGS from the French research ministry. CG thanks Reinhard Zellner for having stimulated the study of the nitrate radicals.

References

1. P. Saxena, L. M. Hildemann, J. Atmos. Chem. **24** (1996) 57.
2. B. Ervens, S. M. Kreidenweis, Environ. Sci. Technol. **41** (2007) 3904.
3. H. Herrmann, Chem. Rev. **103** (2003) 4691.
4. L. Deguillaume, M. Leriche, K. Desboeufs, G. Mailhot, C. George, N. Chaumerliac, Chem. Rev. **105** (2005) 3388.
5. F. Schweitzer, P. Mirabel, C. George, J Phys. Chem. A **104** (2000) 72.
6. R. Sander, Surveys in Geophysics **20** (1999) 1.
7. P. G. de Semainville, D. Hoffmann, C. George, H. Herrmann, Phys. Chem. Chem. Phys. **9** (2007) 958.
8. D. Rousse, C. George, Physical Chemistry Chemical Physics **6** (2004) 3408.
9. C. George, H. El Rassy, J. M. Chovelon, Internat J. Chem. Kin. **33** (2001) 539.
10. C. George, D. Rousse, E. Perraudin, R. Strekowski, Phys. Chem. Chem. Phys. **5** (2003) 1562.
11. X. K. Yang, J. Q. Wang, T. D. Wang, Chin. Chem. Lett. **15** (2004) 583.
12. J. Blanksby Stephen, G. B. Ellison, Acc.Chem. Res. **36** (2003) 255.
13. R. A. Witter, P. Neta, J. Org. Chem. **38** (1973) 484.
14. P. Neta, R. H. Schuler, J. Phys. Chem. **76** (1972) 2673.
15. M. N. Schuchmann, H. P. Schuchmann, M. Hess, C. Von Sonntag, J. Amer. Chem. Soc. **113** (1991) 6934.
16. B. C. Gilbert, J. K. Stell, W. J. Peet, K. J. Radford, J. Chem. Soc., Faraday Transactions 1: Physical Chemistry in Condensed Phases **84** (1988) 3319.

17. M. Exner, H. Herrmann, R. Zellner, Ber. Bunsen-Gesellschaft **96** (1992) 470.
18. R. Zellner, H. Hermann, M. Exner, H. W. Jacobi, G. Raabe, A. Reese, Transport and Chemical Transformation of Pollutants in the Troposphere **2** (1996) 146.
19. J.-P. Le Crane, E. Villenave, M. D. Hurley, T. J. Wallington, J. C. Ball, J. Phys. Chem. A **109** (2005) 11837.
20. B. Cabanas, S. Salgado, P. Martin, M. T. Baeza, E. Martinez, J.Phys. Chem. A **105** (2001) 4440.
21. A. Mellouki, G. Le Bras, H. Sidebottom, Chem. Rev. **103** (2003) 5077.
22. H. Herrmann, A. Tilgner, P. Barzaghi, Z. Majdik, S. Gligorovski, L. Poulain, A. Monod, Atmos. Environ. **39** (2005) 4351.
23. A. Tilgner, Z. Majdik, A. M. Sehili, M. Simmel, R. Wolke, H. Herrmann, Atmos. Environ. **39** (2005) 4389.
24. V. E. Tumanov, E. A. Kromkin, E. T. Denisov, Russian Chemical Bulletin (Translation of Izvestiya Akademii Nauk, Seriya Khimicheskaya) **51** (2002) 1641.
25. C. Walling, G. M. El-Taliawi, J. Amer. Chem. Soc. **95** (1973) 844.
26. S. R. Logan, J. Chem. Soc., Perkin Transactions 2: Physical Organic Chemistry (1972–1999) (1989) 751.
27. S. Gligorovski, D. Rousse, C. H. George, H. Herrmann, Int. J. Chem. Kin. **41** (2009) 309.